Structure of the metallic ζ-phase of oxygen and isosymmetric nature of the ε-ζ phase transition: *Ab initio* simulations

Yanming Ma,[1,2] Artem R. Oganov,[1,3,*] and Colin W. Glass[1]
[1]*Laboratory of Crystallography, Department of Materials, ETH Zurich, Wolfgang-Pauli-Strasse 10, CH-8093 Zurich, Switzerland*
[2]*National Laboratory of Superhard Materials, Jilin University, Changchun 130012, People's Republic of China*
[3]*Geology Department, Moscow State University, 119899 Moscow, Russia*
(Received 29 May 2007; published 1 August 2007)

Using *ab initio* evolutionary methodology for crystal structure prediction, we explore metallic structures of oxygen at pressures in the range of 100–250 GPa. Two energetically competitive monoclinic structures of $C2/c$ (4 mol/cell) and $C2/m$ (8 mol/cell) were found as candidates for ζ-O_2. The $C2/m$ structure is our preferred solution, providing slightly lower enthalpy and better agreement with experimental x-ray diffraction (XRD) pattern and Raman frequencies. Our theoretical prediction supports the isosymmetric nature of the ε-ζ transition, in accordance with the suggestion based on the powder XRD measurements [Y. Akahama *et al.*, Phys. Rev. Lett. **74**, 4690 (1995)]. Moreover, we find that at least up to 250 GPa, oxygen remains a molecular solid and there is no post-ζ-phase in this pressure range.

DOI: 10.1103/PhysRevB.76.064101 PACS number(s): 64.70.Kb, 61.50.Ks, 62.50.+p, 71.15.Mb

I. INTRODUCTION

Oxygen is in many ways a unique element: As the only known elemental molecular magnet, it has a very small $1s^2$-core and compact valence orbitals, allowing short double chemical bonds in the O_2 molecule. However, even in the O_2 molecule and in low-pressure solids (e.g., α- and δ-phases), the simple electron-pair model cannot explain the observed magnetism of this molecule containing unpaired bonding electrons. The collapse of magnetism under pressure was suggested by first-principles calculations[1,2] based on density-functional theory (DFT). Recent neutron diffraction measurements[3] have indeed verified the disappearance of magnetic order in oxygen under pressure when the ε-phase is formed. The very recently discovered crystal structure of the ε-phase consists of O_8 clusters[4,5] (referred to as ε-O_8 in the text) and is consistent with the nonmagnetic nature of this phase.[6] Under pressure, unpaired bonding orbitals of the neighboring O_2 molecules overlap, which induces electron pairing and formation of weak intermolecular bonds. Ultimately, orbital overlap leads to metallization. In solid oxygen, metallization is observed at $\sim$100 GPa upon the formation of ζ-O_2.[7,8] Interestingly, ζ-O_2 was found to become a superconductor below 0.6 K,[9] the origins of which are mysterious since its structure is unknown. Also, ζ-O_2 is the only known molecular superconductor.

Before metallization, oxygen adopts three low-pressure polymorphs: $C2/m$ (Refs. 10 and 11) α-phase, $Fmmm$ (Refs. 12 and 13) δ-phase, and $C2/m$ (Refs. 4 and 5) ε-phase. From the measured x-ray diffraction (XRD) profiles,[8] it seemed possible to determine the unit cell parameters of both ε- and ζ-phases. Both cells turned out to be monoclinic and containing eight molecules. Consequently, an isostructural ε-ζ phase transition was suggested. Using single-crystal XRD,[14] it was suggested that the ε-ζ transition is first order, whereas Raman measurement[14] implied the molecular nature of ζ-O_2. Recent Raman measurement[15] up to 134 GPa suggested that the correct structural model of ζ-O_2 should include at least four O_2 molecules in the primitive cell to explain the observed seven Raman peaks (some of which can be an unresolved superposition of two or more modes). However, existing powder and single-crystal XRD data are not sufficient to resolve the crystal structure of ζ-O_2, leaving it a matter of continuing debate.[8,14,15] On the theoretical side, Serra *et al.*[1] simulated compression of the δ-phase using molecular dynamics technique and discovered an orthorhombic $C2mm$ structure as a candidate for ζ-O_2, bypassing the ε-O_8. Then, a distortion into a monoclinic $C2/m$ (2 mol/primitive cell) structure was enforced to find a good agreement with experimental XRD pattern. However, a maximum of "six" Raman-active modes allowed in this $C2/m$ structure is in contrast to the observation of at least "seven" Raman modes.[15] Here, we explore the metallic structures of oxygen in a wide pressure range (100–250 GPa) using a developed approach, merging *ab initio* simulations and a specifically developed evolutionary algorithm for crystal structure prediction[16–18] implemented in the USPEX code.[17] Two competitive lowest-enthalpy structures of $C2/c$ (4 mol/cell) and $C2/m$ (8 mol/cell) for ζ-O_2 were uncovered. The $C2/m$ structure, which is isosymmetric with the ε-O_8 structure, is suggested to be the best candidate structure.

II. METHOD

The *ab initio* evolutionary simulation for crystal structure prediction searches for the structure possessing the lowest free energy at given P/T conditions and is capable of predicting the stable structure of a given compound knowing just the chemical composition. The first generation of structures is produced randomly. All structures are relaxed at constant pressure; the enthalpy was used as fitness function. Discarding the worst (i.e., highest-enthalpy) structures, we produced the new generation from the best 65% of the structures in a given generation. New structures are created by (1) heredity (combining spatially coherent slabs cut from two parent structures in a random direction at random positions and with random thicknesses) and (2) lattice mutation. In

addition, the best structure of a generation is carried over into the next generation. The evolutionary search was done with the USPEX code,[16–18] and the underlying *ab initio* structure relaxations were performed using DFT with the generalized gradient approximation (GGA),[19] as implemented in the VASP code.[20] The all-electron projector augmented wave[21,22] (PAW) method was adopted, with the PAW potential treating $1s^2$ as core. We used the plane-wave kinetic energy cutoff of 800 eV, which was shown to give excellent convergence of the total energies, energy differences, and structural parameters. For computational convenience, we do calculations at $T=0$ K; thus, the free energy reduces to the enthalpy. The evolutionary structure prediction method has been successfully tested on a large number of different systems and resulted in several predictions at high pressures.[16–18] Zone-center phonon frequencies were calculated within density-functional perturbation theory[23,24] using the Quantum-ESPRESSO package.[25]

III. RESULTS AND DISCUSSIONS

We performed variable-cell structure prediction simulations using the above evolutionary methodology for systems containing two, three, four, six, and eight molecules in the simulation cell at 60, 130, and 250 GPa, respectively. At 130 GPa, two *C*-centered monoclinic structures, $C2/m$ (8 mol/cell) (referred to as ζ-$C2/m$ in the text) and $C2/c$ (4 mol/cell) (Ref. 26) with very similar enthalpies were found to be the most stable. Enthalpy of the $C2/c$ structure is only 2 meV/mol higher than that of ζ-$C2/m$. It is noteworthy that the calculated enthalpies of ζ-$C2/m$ at 130 GPa are 6.4 and 55.2 meV/mol lower than those of $C2mm$ and ε-O_8 structures, respectively, as shown in Fig. 1.[27] Accidentally, ζ-$C2/m$ is isostructural with ε-O_8 and also contains the $(O_2)_4$ clusters, as depicted in the inset of Fig. 1. However, for ζ-$C2/m$, the distance between the $(O_2)_4$ clusters becomes shorter than the intermolecular distance within the cluster, which enables metallic conductivity. Specifically, at 130 GPa, the intercluster distance x_1 (2.009 Å) along the *b* axis in ζ-$C2/m$ is shorter than the intermolecular distance x_2 (2.038 Å) inside the $(O_2)_4$ cluster, while x_1 (2.068 Å) is larger than x_2 (1.937 Å) for ε-O_8. Therefore, the formation of ζ-$C2/m$ is attributable to the shortening of the *b* axis and elongation of the *a* axis in ε-O_8. The calculated band structure [Fig. 2(c)] at 100 GPa clearly reveals the metallic nature of ζ-$C2/m$. Importantly, it is found that ε-O_8 at 40 GPa [Fig. 2(a)] is an insulator with an indirect band gap (Γ-A) of 0.19 eV, while the formation of ζ-$C2/m$ induces a band gap closure [Fig. 2(b)]. Note that the DFT band gap is known to significantly underestimate the true gap. A real band gap closure is expected to occur at much higher pressure. Thus, metallization at the ε-ζ transition is understandable by the scenario of band overlap. Our variable-cell simulations at 250 GPa also predicted the ζ-$C2/m$ and $C2/c$ structures as the most stable ones. Although their enthalpies are too close to be properly distinguished within the accuracy of DFT-GGA theory, present study suggests that there is no post-ζ-phase up to 250 GPa. It is noted that the predicted structures at 250 GPa are still molecular: e.g., for the ζ-$C2/m$ structure, the intramolecular O-O distance is 1.171 Å, much shorter than the shortest intermolecular distance of 1.902 Å.

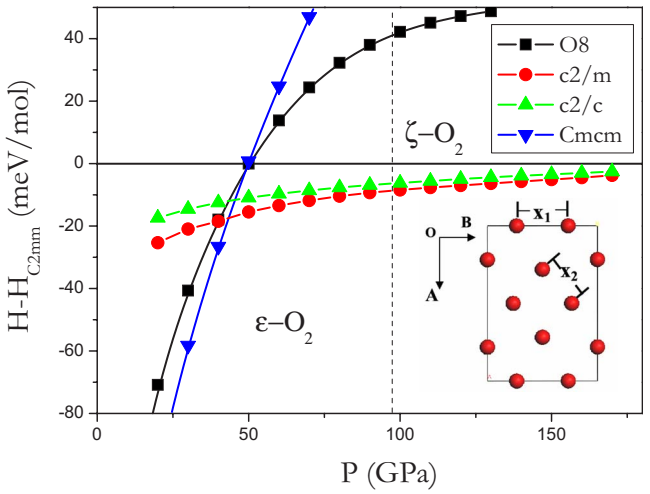

FIG. 1. (Color online) Enthalpies (relative to the $C2mm$ phase) of ε-O_8 (solid squares), ζ-$C2/m$ (solid up triangles), $C2/c$ (solid circles), and *Cmcm* (solid down triangles) phases of oxygen with pressure (Ref. 27). The enthalpy curves are calculated using VASP and the PAW method. Because the enthalpy differences among the structures of *Cmcm*, ε-O_8, $C2mm$, ζ-$C2/m$, and $C2/c$ are rather small, particular care has been taken to ensure the total energy convergence. Structural optimizations were done with a stringent energy convergence tolerance of 1×10^{-5} eV. A very large *k* point set was chosen for the particular structure. Specifically, the *k* point sets for *Cmcm*, ε-O_8, $C2mm$, ζ-$C2/m$, and $C2/c$ are chosen to be $12\times12\times16$, $12\times12\times8$, $12\times20\times8$, $12\times12\times16$, and $16\times16\times8$, respectively. The symbols are the calculated data points. The lines are guides to the eyes. Inset: a schematic representation of ζ-$C2/m$ viewed down along the *c* axis. Label x_1 and x_2 are inter- and intracluster distances, respectively.

Figures 3(a)–3(c) show the calculated equation of state (EOS) and cell parameters (*a*, *b*, *c*, and β) as a function of pressure for ε-O_8 (below 100 GPa) and ζ-$C2/m$ structures (>100 GPa). It is found that except for the small underestimation of β, the current theory reproduces well the experimental data for ε-O_8. It is clear that, though the ε-ζ transition is first order, the discontinuity in the EOS and *c* is very small, while *a* and *b* [Fig. 3(b)] show abrupt increase and decrease, respectively. Note that the experimental β for ε-O_8 [Fig. 3(c)] supposed a sharp decrease at the transition. Here, indeed, we predicted a 1.536° drop in β at the transition of ε-O_8 to ζ-$C2/m$. The current prediction of an isostructural phase transition is consistent with the experimental suggestion by Akahama *et al.*[8] The measured nearly continuous EOS and the discontinuities of *a* and *b* are well reproduced in this prediction.

Figures 3(d) and 3(f) show the measured XRD pattern in the pressure range of 88–116 GPa (Ref. 8) and the simulated XRD for ε-O_8 and ζ-$C2/m$ structures at 116 GPa, respectively. One observes that the simulated XRD [Fig. 3(e)] accurately reproduces the experimental profiles for ε-O_8. From the Raman measurement,[15] it was clearly demonstrated that oxygen samples are actually a mixture of ε-O_8 and ζ-O_2 in the pressure range of 96–128 GPa. Therefore, it is more ap-

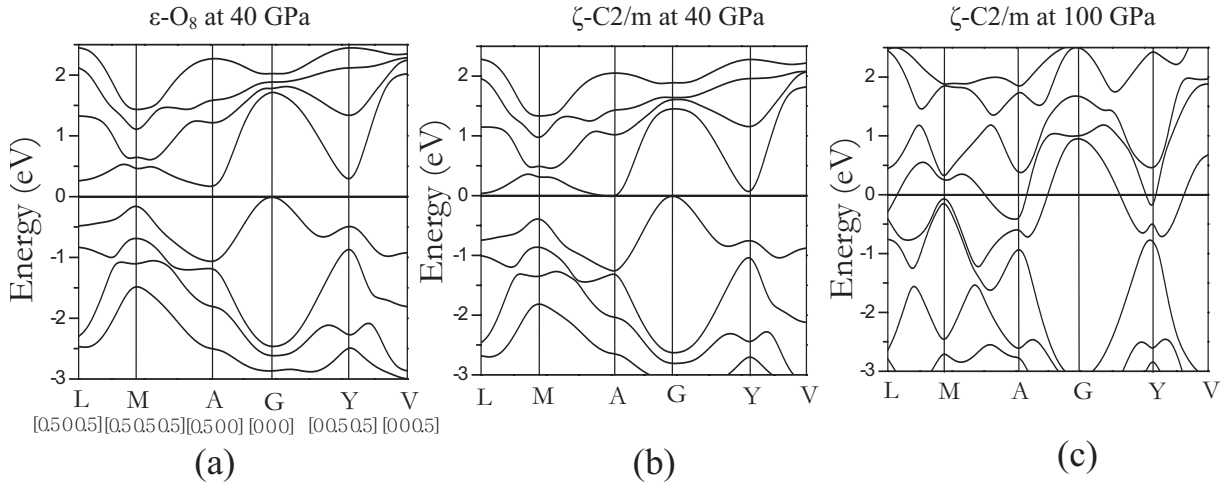

FIG. 2. Band structures for (a) ε-O_8 at 40 GPa and ζ-$C2/m$ at (b) 40 GPa and (c) 110 GPa, respectively, along the symmetric lines of L-M-A-Γ-Y-V.

propriate to understand the measured XRD at 116 GPa [Fig. 3(d)] within the scenario of a two-phase coexistence. At 88 GPa, the experimental XRD of ε-O_8 shows six visible peaks labeled as 1–6. At the ε-ζ transition (96 GPa), the intensities of peaks 1 and 6 start to increase. This behavior might be attributable to the slightly larger intensities of peaks 1 and 6 for ζ-$C2/m$ [Fig. 3(f)]. From Fig. 3(d), it is found that peak 3 starts to lose its intensity and peaks 4 and 5 take over the dominance of intensity with pressure. This XRD feature is understandable by consideration of the weakening of peak 3 in ε-O_8 and the appearance of a stronger peak 4 and a weaker peak 5 in ζ-$C2/m$ at the ε-ζ transition.

Since there are four molecules in the primitive cells of ζ-$C2/m$ and ε-O_8, we have 21 optical modes at zone center: 12 Raman active ($7A_g+5B_g$) and nine infrared active ($4A_u+5B_u$). The pressure dependences of Raman-active modes computed between 80 and 100 GPa for ε-O_8 and between 100 and 150 GPa for ζ-$C2/m$ are plotted in Fig. 4 in com-

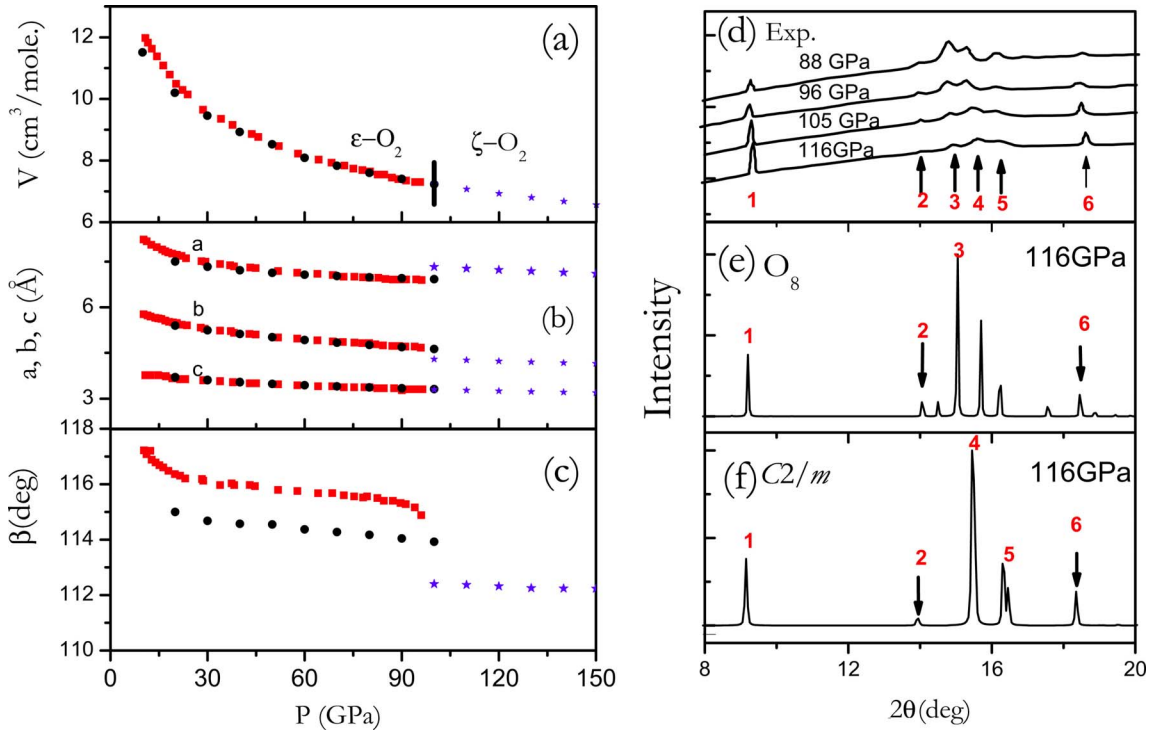

FIG. 3. (Color online) The (a) EOS, (b) lattice parameter a, b, and c, and (c) β for ε-O_8 (below 100 GPa) and ζ-$C2/m$ (>100 GPa) calculated using the Quantum-ESPRESSO code. The red solid squares are the experimental data for ε-O_8. The black solid circles and the blue solid stars are the theoretical results for ε-O_8 and ζ-$C2/m$, respectively. (d) is the experimental XRD data (Ref. 8) at the pressures of 88–116 GPa. (e) and (f) are the simulated XRD patterns for ε-O_8 and ζ-$C2/m$ at 116 GPa, respectively.

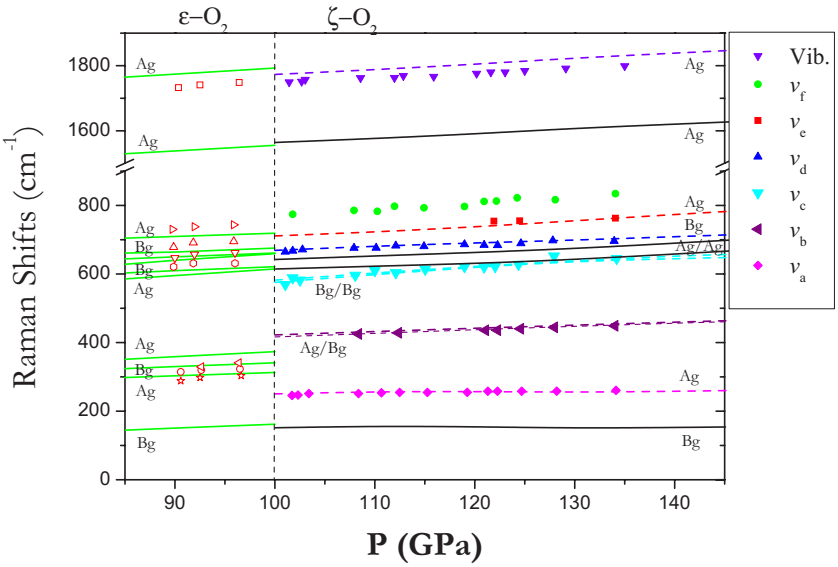

FIG. 4. (Color online) The calculated Raman frequencies (lines) with pressure for ε-O_8 (below 100 GPa) and ζ-$C2/m$ (100–150 GPa). The open and solid symbols are the experimental data (Ref. 15) for ε-O_8 and ζ-O_2, respectively.

parison with the experimental data.[15] It is found that in the frequency range of 200–500 cm^{-1}, the experimentally observed three modes (open left triangles, open circles, and open stars) in ε-O_8 were reduced to two modes (v_a and v_b) with abrupt frequency changes in ζ-O_2. From the significant frequency changes, Goncharov *et al.*[15] concluded that this phase transition is unlikely to be isostructural. However, the current calculations (lines) unambiguously reveal this peculiar feature based on the isostructural phase transition picture (Fig. 4). In theory, the three well separated modes in ε-O_8 are converted into a downshifted mode (A_g) and two almost degenerated upshifted modes (A_g and B_g) due to the charge redistribution upon formation of ζ-$C2/m$. The downshifted mode A_g is attributed to the intermolecular vibration of the $(O_2)_4$ clusters. The formation of ζ-$C2/m$ results in an increased intermolecular distance inside the cluster, thus reducing the Raman frequency. The two upshifted modes A_g and B_g are related to the intermolecular vibration along the shortened b axis. Their near degeneracy precludes an easy observation of two separate Raman-active modes. It is noteworthy that for the vibron, experimental data show a negative discontinuity at the ε-ζ transition. The maximum discontinuity in the vibron is observed to be less than ~1%.[15] The current calculations are also consistent with this feature. The small decrease in the vibron frequency is attributable to the slight increase of the intramolecular bond length from 1.197 Å in ε-O_8 to 1.199 Å in ζ-$C2/m$ at 100 GPa. Note that although the experimental Raman modes of v_a, v_b, and v_c, and vibron in ζ-O_2 are reproduced remarkably well by this theory, the theoretical description of v_d, v_e, and v_f modes between 600 and 800 cm^{-1} is less satisfactory and shows an overall underestimation. Notably, the underestimation is also found in the ε-O_8 structure in this frequency range.

In our previous work,[16] the most stable structure at 25 GPa is predicted to be *Cmcm*, which consists of zigzag chains made of O_2 molecules. This structure is the same as the one previously predicted by Neaton and Ashcroft[2]. Subsequent experiments found a different structure of ε-O_8 (Refs. 4 and 5) at this pressure. However, it should be noted that the predicted chain structure is 22 meV/mol lower in enthalpy (Fig. 1). With increasing pressure, the ε-O_8 structure becomes more favorable than *Cmcm* only above 50 GPa, but less stable than ζ-$C2/m$ and $C2/c$ structures. The calculated enthalpies of ζ-$C2/m$ and $C2/c$ at 60 GPa (Ref. 28) are 27.2 and 23.6 meV/mol lower than that of ε-O_8 (Fig. 1). It is gratifying to confirm that, within a chosen theoretical approximation (here, DFT-GGA), the USPEX method does produce the lowest-enthalpy structure. However, the fact that the most stable structure predicted by theory does not match the experimentally determined structure can have several explanations: (i) the observed ε-O_8 phase is metastable, or (ii) it is thermally stabilized (present calculations are done at 0 K), or (iii) DFT-GGA theory is inadequate for the description of ε-O_8. The first possibility seems unlikely, as crystals of ε-O_8 were produced both by room-temperature compression[29] and growth from the melt.[5] The second possibility cannot be ruled out but requires further experimental studies of the P-T phase diagram. Since the structure of ε-O_8 was solved at 300 K,[4,5] it is conceivable that the entropic effects at 300 K could overturn the 22 meV/mol enthalpy advantage of *Cmcm* over ε-O_8. More problematic is that the ε-ζ transition is observed at 96 GPa (Ref. 8) but is predicted to occur at just ~40 GPa (Fig. 1). This requires the $T\Delta S$ term in the free energy to be ~50 meV/mol at 100 GPa and 300 K. If the third possibility is realized, ε-O_8 could be used as a test bed for the development of improved approximate exchange-correlation functionals beyond DFT-GGA. Earlier, the ferromagnetic bcc phase of Fe played a similar role: its stability could not be explained with DFT-LDA level and required higher-level approximations, and only with the advent of DFT-GGA functionals a correct description could be made. While the reasons of failure of DFT-LDA for bcc-Fe are well understood, the extent and origins of failings of DFT-GGA for ε-O_8 remain to be clarified. It is likely that van der Waals interactions (known to be unsatisfactorily modeled at the DFT-GGA level of theory) are not the main source of errors, since lattice parameters of ε-O_8 are reproduced well at this level of theory (Fig. 3). Our understanding is that the $(O_2)_4$ clusters are held together by weak intermolecular covalent bonds:

each O_2 molecule has two unpaired electrons on two molecular π orbitals, and sharing these electrons with neighboring molecules creates two long intermolecular bonds per molecule and a nonmagnetic ground state. It is well known that DFT-GGA does not perform well for stretched covalent bonds. The origins of these shortcomings are rooted in the self-interaction error and in the locality of the exchange-correlation hole in DFT-GGA, whereas the true exchange-correlation hole in such cases is highly delocalized. At high pressure, intermolecular distances decrease, the intermolecular bonds become more similar to normal covalent bonds, and the true exchange-correlation hole becomes more localized, making DFT-GGA more accurate for ζ-O_2 than it is for ε-O_8. Indeed, our results show good performance of DFT-GGA for ζ-O_2.

ACKNOWLEDGMENTS

We thank the Swiss National Science Foundation (Grant No. 200021-111847/1), CSCS and ETH Zurich for supercomputers, and I. N. Goncharenko for discussions.

*Corresponding author: a.oganov@mat.ethz.ch

[1] S. Serra, G. Chiarotti, S. Scandolo, and E. Tosatti, Phys. Rev. Lett. **80**, 5160 (1998).
[2] J. B. Neaton and N. W. Ashcroft, Phys. Rev. Lett. **88**, 205503 (2002).
[3] I. N. Goncharenko, Phys. Rev. Lett. **94**, 205701 (2005).
[4] H. Fujihisa, Y. Akahama, H. Kawamura, Y. Ohishi, O. Shimomura, H. Yamawaki, M. Sakashita, Y. Gotoh, S. Takeya, and K. Honda, Phys. Rev. Lett. **97**, 085503 (2006).
[5] L. F. Lundegaard, G. Weck, M. I. McMahon, S. Desgrenier, and P. Loubeyre, Nature (London) **443**, 201 (2006).
[6] We performed non-, ferro-, and antiferromagnetic structural optimizations and total energy calculations of ε-O_8 at 17.6 GPa based on the structural parameters of Lundegaard *et al.* (Ref. 5). These calculations suggest a nonmagnetic ground state for ε-O_8.
[7] S. Desgreniers, Y. K. Vohra, and A. L. Ruoff, J. Phys. Chem. **94**, 1117 (1990).
[8] Y. Akahama, H. Kawamura, D. Hausermann, M. Hanfland, and O. Shimomura, Phys. Rev. Lett. **74**, 4690 (1995).
[9] K. Shimizu, K. Suhara, M. Ikumo, K. Amaya, and S. Endo, Nature (London) **393**, 767 (1998).
[10] R. A. Alikhanov, Sov. Phys. JETP **18**, 556 (1964).
[11] C. S. Barrett, L. Meyer, and J. Wasserman, J. Chem. Phys. **47**, 592 (1967).
[12] D. Schiferl, D. Cromer, L. Schwalbe, and R. Mills, Acta Crystallogr., Sect. B: Struct. Sci. **39**, 153 (1983).
[13] F. A. Gorelli, M. Santoro, L. Ulivi, and M. Hanfland, Phys. Rev. B **65**, 172106 (2002).
[14] G. Weck, P. Loubeyre, and R. LeToullec, Phys. Rev. Lett. **88**, 035504 (2002).
[15] A. F. Goncharov, E. Gregoryanz, R. J. Hemley, and H. K. Mao, Phys. Rev. B **68**, 100102(R) (2003).
[16] A. R. Oganov and C. W. Glass, J. Chem. Phys. **124**, 244704 (2006).
[17] C. W. Glass, A. R. Oganov, and N. Hansen, Comput. Phys. Commun. **175**, 713 (2006).
[18] A. R. Oganov, C. W. Glass, and S. Ono, Earth Planet. Sci. Lett. **241**, 95 (2006).
[19] J. P. Perdew, K. Burke, and M. Ernzerhof, Phys. Rev. Lett. **77**, 3865 (1996).
[20] G. Kresse and J. Furthmüller, Phys. Rev. B **54**, 11169 (1996).
[21] P. E. Blöchl, Phys. Rev. B **50**, 17953 (1994).
[22] G. Kresse and D. Joubert, Phys. Rev. B **59**, 1758 (1999).
[23] S. Baroni, P. Giannozzi, and A. Testa, Phys. Rev. Lett. **58**, 1861 (1987).
[24] P. Giannozzi, S. de Gironcoli, P. Pavone, and S. Baroni, Phys. Rev. B **43**, 7231 (1991).
[25] S. Baroni, A. Dal Corso, S. de Gironcoli, P. Giannozzi, C. Cavazzoni, G. Ballabio, S. Scandolo, G. Chiarotti, P. Focher, A. Pasquarello, K. Laasonen, A. Trave, R. Car, N. Marzari, and A. Kokalj, http://www.pwscf.org/. In the structure optimizations and phonon calculations for ε-O_8 and ζ-$C2/m$, the GGA exchange-correlation functional and ultrasoft pseudopotentials are employed. We use the kinetic energy cutoff of 408 eV. We sample the Brillouin zone using the Monkhorst-Pack grid of $10\times10\times12$ for the ε-O_8 structure and $12\times12\times10$ for ζ-$C2/m$.
[26] At 130 GPa, simulations with four and eight molecules produced the ζ-$C2/m$ structure, whereas runs with three and six molecules yielded the $C2/c$ structure. The calculated lattice parameters and atomic positions for ζ-$C2/m$ are $a=7.207$ Å, $b=4.188$ Å, $c=3.232$ Å, $\beta=67.909°$, O1 (0.2056, 0, 0.1984), O2 (0.2725, 0, 0.8011), and O3 (0.0335, 0.2601, 0.8015). The lattice parameters for $C2/c$ are $a=6.119$ Å, $b=2.077$ Å, $c=6.445$ Å, and $\beta=146.515°$; O atoms occupy the 8f Wyckoff position (0.0651, 0.0320, 0.2158).
[27] Interestingly, when we optimized the ε-O_8 structure above 50 GPa using VASP and the PAW method, the ε-O_8 structure spontaneously transforms to the currently predicted ζ-$C2/m$. However, if we use the Quantum-ESPRESSO code and pseudopotential (PP) method to optimize ε-O_8, there is no such spontaneous transition. Note that before 50 GPa, the optimized parameters for the ε-O_8 using PAW and PP methods gave practically identical results. Therefore, in order to simulate the physical behavior of the ε-O_8 through the whole pressure range of 8–96 GPa, we use PP method to optimize its structure. Then, for the enthalpy curve calculation of ε-O_8, we adopt the PP optimized structural parameters to calculate the total energy by PAW method.
[28] At 60 GPa, instead of the ε-O_8 structure, our variable-cell structure prediction simulations also predicted the same two energetically favorable monoclinic structures ζ-$C2/m$ and $C2/c$ as in the simulations at 130 and 250 GPa.
[29] M. Nicol, K. R. Hirsch, and W. B. Holzapfel, Chem. Phys. Lett. **68**, 49 (1979).